Quantum Transport in Conductive Bacterial Nanowires

William Livernois
Department of Electrical and
Computer Engineering
University of Washington
Seattle, WA, USA
willll@uw.edu

M. P. Anantram

Department of Electrical and

Computer Engineering

University of Washington

Seattle, WA, USA

anantmp@uw.edu

Abstract— The electrical properties of conductive heme-based nanowires found in the pili in Geobacter sulfurreducens bacteria were investigated using a density functional theory (DFT) model. Green's function methods were used to calculate quantum transmission and single molecule conductance in both the low temperature (coherent) and room temperature (decoherent) regimes. Several approaches were attempted for modeling the energy levels of the heme-sites, including semi-empirical methods, and quantum transmission was calculated at several different length scales. This result was compared to experimental findings as well as other modeling results for similar cytochrome structures, such as electron hopping models applied to neighboring heme sites. The results show that coordinated hemes prefer a low spin state with electron delocalization over the porphyrin rings and coordinating histidine groups from the protein scaffold. Orbital overlap between heme centers was shown to have a significant impact on quantum transport, with perpendicular heme centers having a rate limiting effect on transport. Semi-empirical models such as the extended Hückel method were found to be inaccurate for modeling transport, showing the importance of electron-electron repulsion and a more detailed model for the organometallic bonding.

Keywords— Density functional theory, bioelectronics, nanodevices, nanomaterials, quantum transport

I. INTRODUCTION

The use of biological structures for charge transport in electronics shows promise for a wide array of applications including nanoelectronics and biosensors. Recent studies have shown that the pili in G. sulfurreducens bacteria have metalliclike behavior, showing functionality as nanowires with high conductivity [1]. Specifically, this conductivity comes from charge transport through the OmcS protein, which consists of heme porphyrins stacked with alternating orientations along a helix protein scaffold as shown in Figure 1. On the cellular level, cytochromes have biological significance as catalysts for redox reactions and charge transport across the cell membrane. These proteins use the cofactor heme, which contains a coordinated porphyrin-iron complex, as the active site for these ionic reactions. Of particular interest are the multi-heme cytochromes involved in extracellular electron transport, which have shown to have transport length scales on the order of microns [2]. The resulting nanowires can have remarkable conductivities and

understanding the electronic properties of these materials can shed light on their future integration into nanoelectronics.

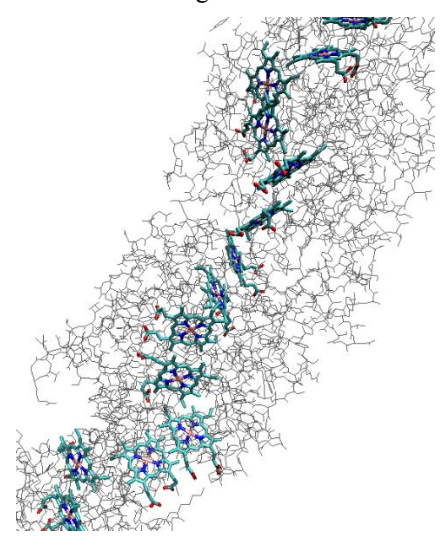


Fig. 1. The structure of the OmsC protein highlighting the location of the heme porphyrin sites.

Previous studies have modeled charge transport in cytochromes using Marcus theory, which combines modeling methods with a semi-classical electron hopping model that uses transitions states to determine rate kinetics [3]. Using this method, each charge site is modeled in its donor or acceptor state to determine rate constants that can be solved as a system of equations to determine the current. Density functional theory (DFT) methods can be combined with other empirical methods to determine the orbital overlap between each site as a part of the rate model. While these results match up with predictions based on similar systems, the high conductivity and metallic-like behavior of the G. sulfurreducens nanowires suggests contributions from coherent quantum transport rather than just incoherent hopping models. Using the quantum transmission spectrum, it is possible to match the experimental conditions used to measure conductivity of the OmcS nanowires by including the interactions with the electrical contacts as well as decoherence.

II. METHODS AND MODELING APPROACH

In this study we have modeled coherent quantum transport starting with the Hamiltonian of the isolated system and using Green's functions to model interactions with the electrical contacts to the system. A mixed basis of localized Gaussian-type orbitals was used with the Gaussian 16 software package [4] to optimize the molecular structure and generate the system Hamiltonian. Using the Green's function method electrical contacts were represented by broadening functions that contain self-energy coupling parameters which can be tuned for a given system based on its interactions with the environment. Using this formalism, the transmission and conductance spectrum of a two terminal nanodevice can be generated using the coupling parameters to simulate electrical contacts on the given molecule.

All DFT calculations were done using the B3LYP hybrid functional with a mixed basis to determine the system Hamiltonian. The LANL2DZ basis with the effective core potential [5] was used to model the Fe atoms in the heme center and the 6-31G** Pope basis set [6] was used to model all other atoms. An unrestricted spin-DFT model was used to verify the spin multiplicity of the ground states. To account for water solvent effect, the polarizable continuum model (PCM) was applied to change the dielectric behavior of the aqueous environment [7]. As a first step, the geometry and bandgap of isolated heme porphyrin was obtained by full structure DFT energy minimization for comparison with the nanowire heme sites. Then, the nanowire structure was modeled in sections ranging from one heme site to a monomer unit consisting of six heme sites. In the pili structure this repeating monomer unit forms the main conductive pathway of the helix structure. The heme sites were modeled including the beta-carbon terminated histidines, which coordinate the Fe center, and cysteine functional groups, which are chemically bonded to the porphyrin ring. This simplified system representation was adapted from other cytochrome DFT studies that showed minimal interaction with surrounding protein [8]. The formation energy of this simplified structure was negative for the single heme case. indicating that this representation was favorable for transport studies. In each nanowire sub-unit, the atomic coordinates of non-hydrogen atoms were held fixed at locations obtained directly from the cryo-EM results and hydrogen locations were optimized by minimizing the total energy at the semiempirical PM6 level [9]. The resulting structure was held fixed, and the total energy was calculated using UHF DFT to determine the spin multiplicity.

To assess the accuracy of semi-empirical methods, the generated system Hamiltonian was compared to the ab-initio DFT results. Starting with the hydrogen location optimized structure, results from the DFT Hamiltonian was compared to two semi-empirical methods: the extended Hückel method [10] and the PM6 method previously mentioned. The energy levels and molecular orbital shapes were compared for each method, looking at the relative HOMO/LUMO gap and the electron density across heme sites. In a second study the protein termination was modified between two structures, comparing beta-carbon terminated histidine and cysteine functional groups with fully connected peptide chains between heme centers. Though the full protein structure was not included in this comparison, every peptide chain connecting the hemes in the

three heme sub-unit was included to check if the protein backbone had any contribution to quantum transmission. For this comparison, the energy levels and transmission spectra were compared to determine the influence of the protein backbone on electron transmission.

For transport calculations, the Green's function method was applied to the system Hamiltonian generated from the Fock and Overlap matrices which used a unitary Löwdin transformation to convert to an orthogonal atomic orbital basis set. The transmission spectrum was determined using the retarded Green's function given by

$$[EI - (H + \Sigma_L + \Sigma_R + \Sigma_R)]G^r = I \tag{1}$$

where E is the energy, H is the system Hamiltonian, $\Sigma_{L/R}$ is the left/right contact retarded self-energy, and Σ_B is the retarded self-energy of the phase breaking decoherence probes that are used to model decoherence in the system [11]. Further, atomic partitioning was used to model decoherence following reference [12]. For each of these self-energy matrices the wide-band limit (WBL) approximation is used, which ignores the real part of the matrices and treats them as energy independent parameters defined at each atom at the contact [13]. The left and right contact self-energies are given by $\Sigma_{L/R} = -i\Gamma_{L/R}/2$ and the decoherence probe self-energies are defined similarly as $\Sigma_{B.n} = -i\Gamma_n/2$ for each of the n probes. Using the Greens function we can define the transmission between probes n and m to be

$$T_{nm}(E) = Trace[\Gamma_n G^r \Gamma_m (G^r)^{\dagger}]$$
 (2)

where probe n and m are inclusive of the left/right electrical contacts and decoherence probes. The current flowing through probe n is given by the Buttiker formula,

$$I_n = \frac{2q}{h} \sum_m \int T_{nm}(E) [f_n(E) - f_m(E)] dE$$
 (3)

where $f_n(E) = 1 + \exp\left(\frac{E - E_{f,n}}{K_b T}\right)$ is the Fermi distribution defined at probe n. Since the current at each decoherence probe is zero at every energy and current only flows between the left and right contacts, the transmission between the left and right contacts can be simplified to give

$$T_{eff} = T_{LR} + \sum_{n} \sum_{m} (T_{Ln} W_{nm}^{-1} T_{mR})$$
 (4)

where n and m are summed over the decoherence probe sites and W_{nm}^{-1} is the inverse of $W_{nm} = (\sum_{n \neq m} T_{nm}) \delta_{nm} - T_{nm} (1 - \delta_{nm})$, an operator that propagates scattering at each probe site. The first term in equation (4) defines the coherent transport while the second accounts for decoherence. From this transmission the zero-bias conductance can be calculated by taking the derivative of (3) with respect to the applied bias (chemical potential difference divided by q) and plugging in (4) to get

$$G(E_f) = \frac{2q^2}{h} \int T_{eff}(E) \frac{\partial f(E - E_f)}{\partial E} dE.$$
 (5)

In the low temperature limit, the derivative of the Fermi function can be modeled as a delta function, meaning that the low-bias conductance at a certain Fermi energy can be approximated as the transmission times the quantum of conductance. This approximation was used for comparison to experimental results, looking at decoherent and fully coherent

transmission to determine the applicability of each model at different length scales.

III. RESULTS

A. Single Heme Unit

A single heme-B molecule was modeled without protein coordination as a baseline study. Modeling this with different spin states showed that Fe center preferred a high spin state, with the resulting system energy showing a minimum in the triplet state. A band gap of 2.9 eV was found for the neutral heme-B results with the HOMO and LUMO orbitals completely delocalized over the resonant porphyrin structure. Upon adding two coordinating histidine groups to the Fe center and bonded cysteines, as present in the full nanowire structure obtained from cryoEM [2], the singlet state (no spin) was energetically preferred for this neutral structure. This preference matches up with previous studies where the spin alignment energy competes with ligand field splitting caused by the presence of the histidine ring [14]. The coordinated structure in the singlet state had a band gap of 2.67 eV with HOMO and LUMO orbitals delocalized over the resonant heme structure and histidine rings.

B. Two and Three Heme Sub-units

The full OmcS protein consists of alternating parallel and perpendicular heme pair arrangements and these geometries were compared as the basic building blocks of the nanowire structure. As in the single heme case, the singlet state was confirmed to be energetically preferred for both geometries. Between the two geometries the perpendicular conformation showed a much lower orbital overlap, and the resulting transmission was found to decrease by at least a factor of 10 as shown in Figure 2. In the three-heme case, the HOMO and LUMO orbitals showed full delocalization over parallel stacked hemes while only some electron density was found on the perpendicular heme at the edge of the porphyrin and at the Fe center. Fully coherent transmission across the three heme subunit was found to decrease by several orders of magnitude when compared with the perpendicular heme case. Adding decoherence probes to the model increased transport significantly within the HOMO and LUMO energy bands, which contained tightly packed quasi-degenerate energy states.

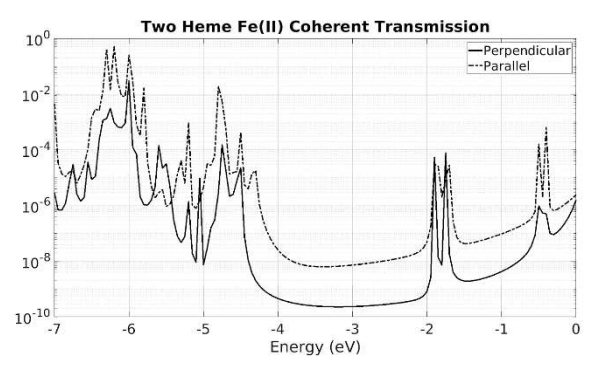


Fig. 2. Coherent transmission spectrum of the two heme sub-unit as a function of Fermi energy for the perpendicular and parallel pair conformations

C. DFT Model Accuracy Studies

The Hamiltonian generated from the semi-empirical results showed significant divergence from the ab-initio DFT results.

Both semi-empirical methods have been shown to give good approximations for orbital shape and energy levels for organic systems, with the PM6 method specifically showing high agreement for protein structure when compared to crystallization results [15]. However, for the case of the OmcS cytochrome structure, both methods show major differences in energy levels from the full B3LYP DFT calculation as shown in Figure 3. This was especially true near the band gap for the heme structure, likely because of the d-orbital interactions from the iron center. The results from the extended Hückel method, which does not include any d-orbital modeling, shows no band gap in the multi-heme structure and complete delocalization of the metal-like energy band across all heme porphyrin centers. While the PM6 method does include an improved model for transition metal atoms, the resulting band gap of the material increases dramatically to 5.1eV with the HOMO and LUMO orbitals showing up highly localized at individual heme porphyrins. The full DFT calculation with a mixed basis and hybrid functional falls somewhere between these methods, showing some delocalization of HOMO and LUMO orbitals that increases as a function of the oxidation state and a moderate band gap.

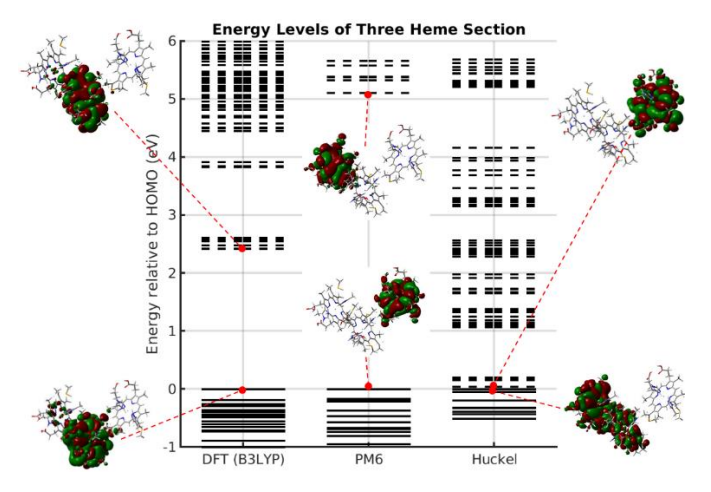


Fig. 3. Comparison of energy level distribution for ab-initio DFT and semiempirical methods, showing an isosurface visualization of the HOMO and LUMO orbitals for each case ($|\psi|$ =0.002, colored by wavefunction sign)

Comparison of the transmission of the three heme sub-unit with and without connect peptide chains is shown in Figure 4 (a). While the energy levels approximately line up between the structures relative to the HOMO energy, the density of states at the bottom of the LUMO band increases in the case of the betacarbon terminated structure. This can also be seen in a comparison of the transmission, indicating that at this energy level the peptide chain has some influence on transmission pathways through the structure. For all other energies, the betaterminated structure showed similar peaks and was an underestimate of the transmission with the peptide chains.

Using the transmission spectrum, it is possible to get a range of low-bias conductance values to compare to the experimental results as described in Equation 5. Based on the results from [2], the experimentally measured conductance linearly scaled to the six-heme unit would be $2.4E-4G_0$, where G_0 is the quantum of conductance. Applying electron hopping models to this structure

has greatly underestimated this conductance value due to the low electron coupling values between neighboring hemes, and it has been suggested that other transport models must be used to explain this conductivity [16]. Using our decoherent model, our conductivity values range from $1.4E-7G_0$ for fermi energies in the band gap to $1.7E-4G_0$ for fermi energies near the LUMO as shown in Figure 4. This greatly exceeds the conductance values determined by purely coherent transport which would have a maximum possible value of $1.8E-5G_0$ based on the peak coherent transmission values between parallel hemes (see Figure 2). While the range of transmission values in both examples span several orders of magnitude, highly dependent on the Fermi energy relative to the HOMO and LUMO levels, they provide a bound to the limits of quantum transmission in the structure.

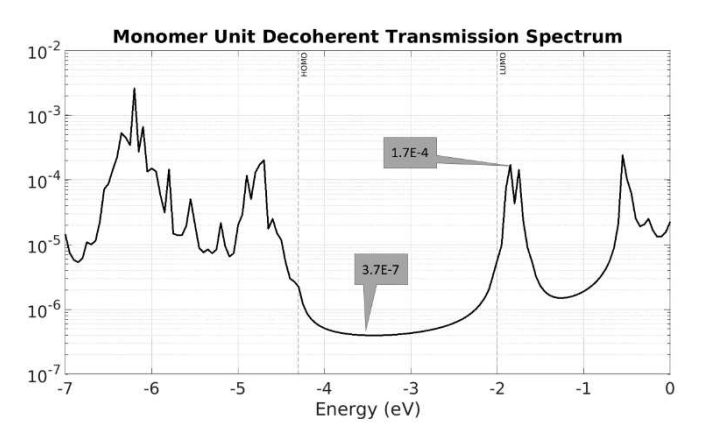
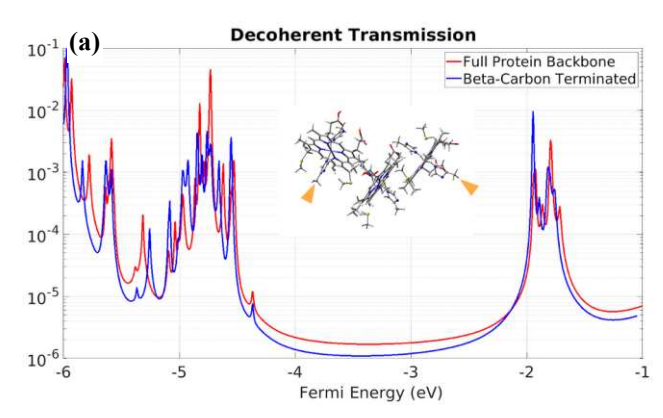


Fig. 4 Decoherent ransmission spectra of the full monomer unit (six heme sites) with labels corresponding to the minimum transmission in the bandgap and maximum transmision peak in the LUMO band.

IV. DISCUSSION AND CONCLUSIONS

The results from our mixed-basis DFT model match up well with previous computational studies and experimental results with cytochrome structures. Figure 5(a) shows minimal differences in decoherent transmission between the fully connected peptide structure and beta-carbon terminated ligands. which indicates that this structure approximation was a valid assumption and quantum transmission mainly occurred between coordinated hemes. Semi-empirical models were shown to be highly inaccurate for modeling the organometallic heme sites, especially for the transport calculations used in this study that rely upon accurate band energies and density of states. This is especially demonstrated for the case of purely coherent transmission, where the extended Hückel method generates highly irregular results as shown in Figure 5(b). While the resulting Hamiltonian of the ab-initio DFT model did not show metallic behavior, the band gap of the system did noticeably decrease with the addition of the coordinated histidine rings and multiple hemes sites. In addition, the density of states near the HOMO and LUMO energies was large, leading to higher transmission as the Fermi energy approached these energy values.



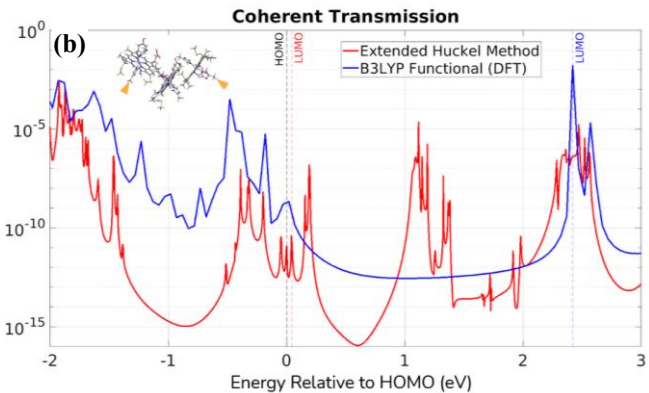


Fig. 5 Transmission spectra of the three-heme subunit comparing (a) the decoherent transmission spectrum of the fully connected peptide backbone and beta-terminated structures and (b) coherent transmission of the ab-initio DFT and extended Hückel methods, inset images show contact locations

Adding a decoherence model to the system allowed the energy levels to broaden as a representation of the energy fluctuations seen in a biological system. While previous studies show that mixing coherent and incoherent models can help account for some of this behavior [16], these models still assume that electrons occupy discrete set of states using constant hopping rates. The decoherence model used in this study allowed usage of a single minimized snapshot of the system to represent the time-average behavior and any energy fluctuations as a broadening function applied at each decoherence probe. This was especially important for the larger structures, where energy levels are very closely spaced and small fluctuations in local energy can have a profound impact on quantum transport. Adding in the decoherence model using energy independent broadening at each atom, the transmission was found to increase as the Fermi energy approached the HOMO and LUMO energies.

The decoherent transmission was linearly dependent on system size, indicating that the length scales of the heme spacing were longer than the ballistic transport limit in the model. To get a full picture of the quantum transport between heme sites, further investigation of different oxidation states will need to be included, especially due to the low redox potential of the Fe center and low disassociation energies found in some of the organic functional groups. Even for the neutral reduced state, we have demonstrated the significance of decoherent quantum

transport as a leading mechanism for electron conduction in OmcS nanowires.

ACKNOWLEDGMENT

This work is funded by National Science Foundation Grant Number FMSG ECCS - 2036865 and National Defense Science and Engineering Graduate Fellowship. This conducted using the advanced computational, storage, and networking infrastructure provided by the HYAK supercomputing cluster at the University of Washington. We thank Dr. Walid Hassan for pointing out the importance of triplet states.

REFERENCES

- [1] N. S. Malvankar, M. Vargas, K. P. Nevin, A. E. Franks, C. Leang, B.-C. Kim, K. Inoue, T. Mester, S. F. Covalla, J. P. Johnson, V. M. Rotello, M. T. Tuominen, and D. R. Lovley, "Tunable metallic-like conductivity in microbial nanowire networks," Nature Nanotechnology, vol. 6, no. 9, pp. 573–579, 2011.
- [2] F. Wang, Y. Gu, J. P. O'Brien, S. M. Yi, S. E. Yalcin, V. Srikanth, C. Shen, D. Vu, N. L. Ing, A. I. Hochbaum, E. H. Egelman, and N. S. Malvankar, "Structure of Microbial Nanowires Reveals Stacked Hemes that Transport Electrons over Micrometers," Cell, vol. 177, no. 2, 2019.
- [3] R. A. Marcus, "On the Theory of Oxidation-Reduction Reactions Involving Electron Transfer. I," J. Chem. Phys., vol. 24, no. 5, pp. 966– 978, 1956
- [4] M. J. Frisch, et al. "Gaussian~16 Revision C.01.", 2016.
- [5] P. J. Hay and W. R. Wadt, "Ab initio effective core potentials for molecular calculations. Potentials for the transition metal atoms Sc to Hg," *The Journal of Chemical Physics*, vol. 82, no. 1, pp. 270–283, 1985.
- [6] G. A. Petersson and M. A. Al-Laham, "A complete basis set model chemistry. II. Open-shell systems and the total energies of the first-row

- atoms," The Journal of Chemical Physics, vol. 94, no. 9, pp. 6081–6090, 1991
- [7] J. Tomasi, B. Mennucci, and R. Cammi, "Quantum Mechanical Continuum Solvation Models," *Chem. Rev.*, vol. 105, no. 8, pp. 2999– 3094, 2005.
- [8] M. Breuer, K. M. Rosso, and J. Blumberger, "Electron flow in multiheme bacterial cytochromes is a balancing act between heme electronic interaction and redox potentials," Proceedings of the National Academy of Sciences, vol. 111, no. 2, pp. 611–616, 2014.
- [9] J. J. P. Stewart, "Optimization of parameters for semiempirical methods V: Modification of NDDO approximations and application to 70 elements," J Mol Model, vol. 13, no. 12, pp. 1173–1213, 2007.
- [10] R. Hoffmann, "An extended Hückel Theory. I. Hydrocarbons," The Journal of Chemical Physics, vol. 39, no. 6, pp. 1397–1412, 1963.
- [11] J. Qi, N. Edirisinghe, M. G. Rabbani, and M. P. Anantram, "Unified model for conductance through DNA with the Landauer-Büttiker formalism," Phys. Rev. B, vol. 87, no. 8, p. 085404, 2013.
- [12] H. Mohammad, B. Demir, C. Akin, B. Luan, J. Hihath, E. E. Oren, and M. P. Anantram, "Role of intercalation in the electrical properties of nucleic acids for use in molecular electronics," *Nanoscale Horizons*, 2021
- [13] C. J. O. Verzijl, J. S. Seldenthuis, and J. M. Thijssen, "Applicability of the wide-band limit in DFT-based molecular transport calculations," The Journal of Chemical Physics, vol. 138, no. 9, p. 094102, 2013.
- [14] D. M. Smith, M. Dupuis, E. R. Vorpagel, and T. P. Straatsma, "Characterization of Electronic Structure and Properties of a Bis(histidine) Heme Model Complex," *Journal of the American Chemical Society*, vol. 125, no. 9, pp. 2711–2717, 2003.
- [15] J. J. Stewart, "Application of the PM6 method to modeling proteins," Journal of Molecular Modeling, vol. 15, no. 7, pp. 765–805, 2008.
- [16] Y. Eshel, U. Peskin, and N. Amdursky, "Coherence-assisted electron diffusion across the multi-heme protein-based bacterial nanowire," Nanotechnology, vol. 31, no. 31, p. 314002, 2020.